Gaussian beams and Fresnel volume elements

Carlos A. S. Ferreira(*), German Garabito(+), Pedro Chira Oliva(+)
(*) Center of Geosciences, Graduation Course in Geology, Federal University of Pará, Brazil
(+) Center of Geosciences, Post-Graduation Course in Geophysics/CPGf, Federal University of Pará, Brazil

This paper was prepared for presentation at the 9th International Congress of the Brazilian Geophysical Society held in Salvador, Brazil, 11-14 September 2005.

Abstract

The Gaussian beam concept was originally introduced in the seismological literature by Russian and by Czech researchers in the beginning of the 80's, in order to investigate certain limitations of the zero order ray theory, up to now the standard method to study the propagation of a seismic wavefield in smooth geological models. This paper investigates then a possible relationship of this concept with the Fresnel volume elements. This restriction permits that certain parameters that control the half-widths of the beams present an analytical expression, based on the knowledge of the Fresnel volume elements, common on modeling of seismic wavefield, and that can be fully determined by dynamic raytracing (DRT).

Introduction

Gaussian beams (GBs) are high-frequency time harmonic solutions of the elastodynamic equation concentrated close to their central rays (Klimeš, 1984). They were introduced in the seismological literature by Popov (1982) and Popov and Psencǐk (1978), based on the works of several Russian researchers, and later developed by Czech researchers on behalf of the "Seismic Waves in Complex 3D Structures" project, at Charles University, Praha. Later, Červený (1982), Popov et al. (1982), Červený and Klimeš (1984), Müller (1984), among others, developed the idea behind which synthetic seismograms could be obtained by a *superposition* of GBs as an asymptotic approximation of the zero order ray theory. This concept had as main characteristic the fact that a superposition of beams could overcome some drawbacks of the seismic wavefield propagation, such as the regularity of the wavefield in singular regions of the assumed known velocity model, the consideration of rays not traced by raytracing codes in shadow zones or more complex geological models, etc. In order to do so, a certain integral representation of complex paraxial GBs had to be introduced, together with the definition of a special weight-function, whose asymptotic determination lead to the zero order ray theory solution. In numerical terms, Klimeš (1984) shed some light upon the use of this weight-function geometrically, by using elements of the ray-centred coordinates propagator matrix, which are well-known solutions of the DRT system. The final result in Klimeš (1984) presented an important *numerical* solution for the weight-function. However, its *physical* significance had not been investigated so far. Since the ray-centred matrices are related to the so called Bortfeld propagator sub-matrices (Bortfeld, 1989), and these latter are related to the calculation of the Fresnel volume elements (Schleicher et al., 2004), it became clear to us that the numerical solution of Klimeš (1984) had also an interpretation in terms of the Fresnel volume elements.

An important aspect in this respect is the fact that, by using the Fresnel volume elements, we are able to assign an analytical representation for certain parameters that control important features of the GBs, such as its half-widths. This has important consequences in terms of stability. Since the beams are very sensitive to the optimal choice of the initial conditions of the (complex) DRT system, the analytical expression for the beam parameters established in this work, in terms of the Fresnel volume elements, guarantee to us that we can control these quantities and avoid artifacts when modeling the wavefield. In particular, the weight-function that we introduce is proportional to the Fresnel zone in depth and/or its counterpart, projected towards the acquisition surface (Schleicher et al., 1997; Schleicher et al., 2004), indicating that the main contribution to a certain observation, in the paraxial meaning, are the ones belonging to points inside the Fresnel zone.

In this work we study the properties of construction of synthetic seismograms with the GB concept in a different manner. We first transform the integration domain of the GBs superposition integral into a more suitable domain for the description of the problem, i.e., over the acquisition surface, where seismic data are gathered, precisely when they are restricted to the Fresnel zones of each trace. In the following, this transformation leads to asymptotically determine the new form of the weight-function and make use of the quantities determined during the DRT. Finally, we test our modeling operator in one seismological example, simulating the propagation of a seismic wavefield in the crust-mantle interface.

The Fresnel volume elements

In order to demonstrate the formation of the Fresnel volume, we shall use the concept of seismic system introduced by Bortfeld (1989). We consider then an arbitrary number of isotropic, homogeneous or inhomogeneous layers, separated by smooth and curved interfaces. According to Hubral et al. (1993) and Schleicher et al. (1997), the Fresnel zones are cross sections of the Fresnel volume (ray tubes), formed by the set of intersection points of paraxial rays over a given (fictitious or not) surface inside the Earth, during its path between a source *S* and a receiver *G*, considering that the traveltime of each paraxial ray does not differ from the traveltime of the central ray, along the same path way, by more than one-half period of the monofrequency wave (Figure 1). Mathematically, this has the following formal definition (Schleicher et al., 1997)

$$\left|\tau_1(S,\overline{M}) + \tau_2(\overline{M},G) - \tau(S,G)\right| \leq \frac{T}{2}. \qquad (1)$$

where τ_1 and τ_2 are paraxial traveltimes for two ray branches, while τ is the traveltime of the central ray and T is the period. Point $\overline{M}$ is a neighbor point of the specular reflection point M_R in depth. These points define a reflection or a transmission surface Σ_F or, more precisely, a tangent plane at the same point. Then the Fresnel volume is defined as the envelope of all Fresnel zones set up along all arbitrary surfaces that intercept a central ray along its pathway between S and G. In other words, Eq. (1) can be rewritten as (Schleicher et al., 1997)

$$\left|\vec{\mathbf{x}}_M . \mathbf{H}_F \vec{\mathbf{x}}_M\right| \leq T \qquad (2)$$

where $\mathbf{H}_F = \mathbf{D}_1\mathbf{B}_1^{-1} + \mathbf{B}_2^{-1}\mathbf{A}_2$ is the 2 x 2 Fresnel zone matrix (Hubral et al., 1993; Schleicher et al., 1997) in terms of the 2 x 2 submatrices of the Bortfeld surface-to-surface propagator matrix (Bortfeld, 1989; Schleicher et al., 1997). Here we have also used the paraxial (parabolic) approximation of the traveltimes in order to get to Eq. (2) (Schleicher et al., 2004).

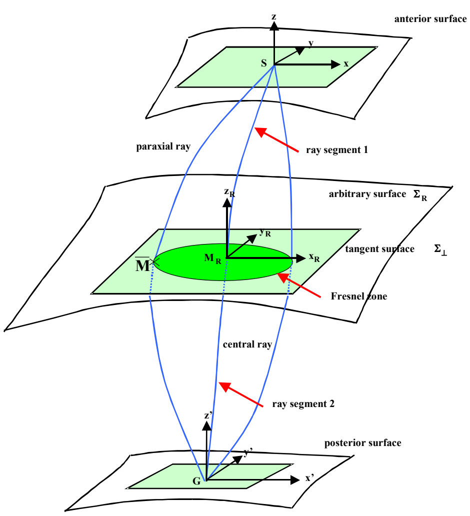

Figure 1 – Fresnel volume and the seismic system (Adapted from Schleicher et al., 2004).

Another important relationship derived from the concept of Fresnel zone is the *projected* Fresnel zone. Geometrically, this zone is a region located at the acquisition surface and that is formed by the set of points that reflected inside the true Fresnel zone over Σ_F (Schleicher et al., 1997). Its formal definition is given by

$$\mathbf{H}_P = \mathbf{\Lambda}^T \mathbf{H}_F^{-1} \mathbf{\Lambda}, \qquad (3)$$

where $\mathbf{\Lambda} = \mathbf{B}_2^{-1}\mathbf{\Gamma}_G + \mathbf{B}_1^{-1}\mathbf{\Gamma}_S$ and Γ_j (j = S, G) is the configuration matrix (Schleicher et al., 1993).

Equations (2) and (3) are all that is necessary from the Fresnel volume elements to be known in order to relate them to GBs. The other relationship is the one involving their definition in terms of the (ray centred) DRT sub-matrices. We shall not present them here. Their definitions can be seen in Červený (2001).

The Gaussian Beam concept

GBs are bell-shaped time-harmonic solutions of the elastodynamic equation, concentrated close to their central rays (Klimeš, 1984). They exist in the paraxial vicinity of a given ray, accompanying them along its whole pathway, whose amplitude are Gaussian decaying with respect to the distance from this central ray, and that form a continuous and coherent beam along the same pathway. They can be described in ray-centred and general Cartesian coordinates (Figure 2). We shall also consider local Cartesian coordinates (Červený, 2001). Its mathematical definition was established in Ferreira and Cruz (2003).

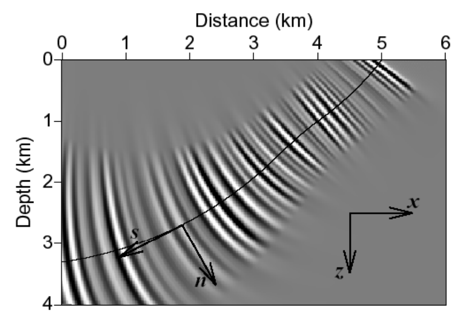

Figure 2 – A Gaussian beam, the ray-centred coordinate system (s, n) and the general cartesian coordinate (x, y) (Hale, 1993).

The most important features of the GBs are that they are complex paraxial rays that are tightly concentrated around the central ray (in a bell-shaped manner), and are regular along its whole pathway, with non-singular amplitudes and no phase shifts. GBs present complex paraxial traveltimes, which leads to the definition of a complex wavefront curvature matrix, whose imaginary part is related to the so called beam half-width. They obey the same initial conditions of the real DRT system (e.g., point source or initial wavefront), but in a complex way, in order to establish a relationship with the half-width. In mathematical terms, the half-width is given in 3D by (Müller, 1984)

$$\mathbf{L}(S,G) = \sqrt{\frac{2}{\omega}\left\{\frac{(\varepsilon_1\mathbf{Q}_1 + \mathbf{Q}_2)^2}{\varepsilon_2} + \varepsilon_2\mathbf{Q}_1^2\right\}} \qquad (4)$$

where $\mathbf{Q}_1$ and $\mathbf{Q}_2$ are 2 x 2 sub-matrices of the ray-centred 4 x 4 propagator matrix Červený (2001) and ω is the angular frequency. They are also complete solutions of the DRT system (Ferreira and Cruz, 2003). The 2 x 2 matrices ε_1 and ε_2 are the real and imaginary components of a complex 2 x 2 matrix $\boldsymbol{\varepsilon}$, respectively. They specify special conditions that must be obeyed by the beams, either at the source or at the receiver, and that control the width of the beams (Müller, 1984). These quantities had been studied so far in a pure empirical and numerical way, the search of its optimal values only granting more stable solutions in the obtaintion of synthetic seismograms. The problem with Eq. (4) and with the parameters ε_1 and ε_2 is that they do not constraint the beam half-width in a precisely physical way, i.e., their numerical values are still insufficient to prevent spurious arrivals or non-physical observations in the synthetic seismograms. Our purpose is to relate Eq. (4) to Eq. (2) in depth and project this values using Eq. (3) towards the acquisition surface and find an analytical expression for the parameters ε_1 and ε_2. Unfortunately, this cannot be done for both quantities: we must specify *some* condition in which more stable results are gathered. The one that had presented more stable results and that is recommended by Müller (1984) is the one in which $\varepsilon_1 = 0$, that is equivalent to grant that the beams at the endpoints of the rays present a half-width with the most possible minimum value.

In order to find an analytical expression for the parameters ε_1 and ε_2, besides the empirical ones discussed by Müller (1984), we shall consider a situation in 2D. This is easily done by considering only the upper right elements of each DRT sub-matrix. By expressing Eq. (2) as an analogue expression using Eq. (3), the size of the projected Fresnel zone in the 2D case can be easily estimated as

$$r_F = \sqrt{\frac{1}{f\,H_P}} \tag{5}$$

where *f* is the dominant frequency of the mono-frequency wave and H_P is the upper right element of Eq. (3). Equating Eq. (5) to Eq. (4), for the case of $\varepsilon_1 = 0$, we are led to a simple second degree equation in ε_2, whose solution is given by

$$\varepsilon_2^{\pm} = \frac{\dfrac{\pi}{H_P} \pm \sqrt{(\dfrac{\pi}{H_P})^2 - 4Q_1^2 Q_2^2}}{2Q_1^2}\,. \tag{6}$$

Eq. (6) tell us that the important beam parameter ε_2 is now calculated based on a known physical quantity, i.e., the projected Fresnel zone value of the wavefield. This formally also restricts the value of ε_2 to the knowledge of the size of the Fresnel zone on the acquisition surface, indicating that infinitely broad GBs are no longer possible at the endpoints of the rays. Only for comparison reasons, if by chance we considered broad projected Fresnel zones sizes, i.e., $H_P \to \infty$, Eq. (6) yields the same result as discussed in Müller (1984). Thus, it means that Eq. (6) is a more restrictive and physical condition for the case of as narrow beams as possible at the endpoints of the rays. The “plus” and “minus” solutions only indicate possible choices of constraint when referred to projected Fresnel zones. But, overall, *physically* speaking, Eq. (6) implies that the GBs half-widths are restricted to the Fresnel volume of the wavefield.

The modeling integral

In the following, we shall study a modified version of the GBs superposition modeling integral discussed in Ferreira and Cruz (2003). Now we consider that the synthetic seismograms are obtained, at the geophone position $\vec{\mathbf{x}}_G(\vec{\xi})$, by the following equation in the frequency domain (Ferreira and Cruz, 2004a,b)

$$\begin{aligned} U(\vec{\mathbf{x}}_G(\vec{\xi}),\omega) = & \int_{A_P} d\,\xi_1^P\, d\,\xi_2^P\, \frac{det\,\mathbf{\Lambda}}{det\,\mathbf{H}_F} \frac{\Phi(\vec{\xi}^P)}{cos\,\theta_G\, det\,\mathbf{Q}(\vec{\xi}^P)}\,. \\ & \times D(\vec{\xi}^P, L)\, A(\vec{\xi}^P) \exp[i\,\omega\, T_R(\vec{\mathbf{x}}_G(\vec{\xi}),\vec{\xi}^P)] \end{aligned} \tag{7}$$

Here, θ_G is the emergence angle at the geophone and $det\,\mathbf{Q}(\vec{\xi}^P)$ is the quantity related to the geometrical spreading, while $A(\vec{\xi}^P)$ is the amplitude, respectively.. In this work, we assume that

$$\Phi(\vec{\xi}^P) = \frac{i\,\omega}{2\pi}\sqrt{det\,\mathbf{H}_F}\,\frac{cos\,\theta_G}{det\,\mathbf{Q}(\vec{\xi}^P)} \tag{8}$$

is the weight-function that asymptotically reduces Eq. (7) to the zero order ray theory solution (Ferreira and Cruz, 2004a,b), while the vector $\vec{\xi}^P = (\xi_1^P, \xi_2^P)^T$ is a subset of the coordinate vector $\vec{\xi}$, that parameterizes the positions of sources and geophones, and which indicates the positions of points inside the projected Fresnel zones. $T_R(\vec{\mathbf{x}}_G(\vec{\xi}),\vec{\xi}^P)$ is the real parabolic paraxial traveltime at the geophone *G*, its position parametrerized by $\vec{\xi}$, due to a observation located at $\vec{\xi}^P$. Finally, we have that

$$D(\vec{\xi}^P, L_{ij}) = \exp\left(-\frac{\xi_i \xi_j}{2L_{ij}^2}\right) \tag{9}$$

is the Gaussian taper function derived from the imaginary part of the traveltime function of the GBs, where L_{ij} are the components of the beam half-width matrix [see Eq. (4)]. By inserting (8) in (7) and coming back to the time domain, after convolving the final equation with the source function $F(\omega)$, we have

$$\begin{aligned} O(\vec{\mathbf{x}}_G(\vec{\xi}),t) = -\frac{1}{2\pi} & \int_{A_P} d\,\xi_1^P\, d\,\xi_2^P \sqrt{det\,\mathbf{H}_P(\vec{\xi}^P)}\, D(\vec{\xi}^P, L) \\ & \times \dot{F}(\vec{\xi}^P, t - T_R(\vec{\mathbf{x}}_G(\vec{\xi}),\vec{\xi}^P)) \end{aligned}\,. \tag{10}$$

This is our final modeling integral. It considers the contributions at geophone *G* of only all those rays that emerge on its projected Fresnel zone on the acquisition surface. By its turn, Eq. (8) represents a strong constraint for the rays: again, only those rays inside the projected Fresnel shall be considered by the summation in Eq. (10).

Seismological example

We shall demonstrate the effective use of the Fresnel volume elements as constraints in the construction of beams, followed by the construction of its synthetic seismograms, in a seismological example. This example depicts the well known fact that *P* waves experiment a strong increase of 6 Km/s to 8 Km/s at the crust-mantle interface, i.e., in the so called Mohorovicic (Moho) discontinuity, where some difference in the physical properties of the Earth are supposed to exist. Then, we have built a velocity profile (Figure 3) in which the crust is initially homogeneous, and experiments, at depth 15 Km (in this case, the base of the Moho), an approximate linear increase in the values of *P* wave velocities.

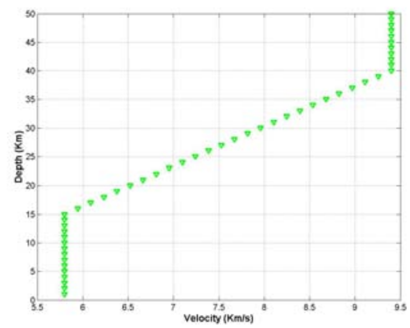

Figure 3 – Velocity profile for the seismological example

In Figure 4b we have the ray diagram for a common-shot experiment, where a source point is located at the origin of a Cartesian coordinate system. This example is based on Červený (1985), where we have used 2 Hz as the dominant frequency signal. We have considered the existence of 40 receivers (seismological stations), each one spaced 5 Km from each other, distributed in line over a distance of 200 Km. The total depth considered was 40 Km.

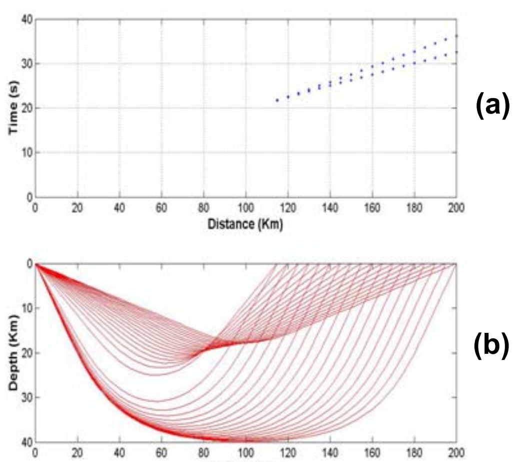

Figure 4 – Traveltime and ray diagram for the seismological example.

In Figure 4a, the traveltime curve presents two divergent branches due to the caustic formation around depth 15 Km.

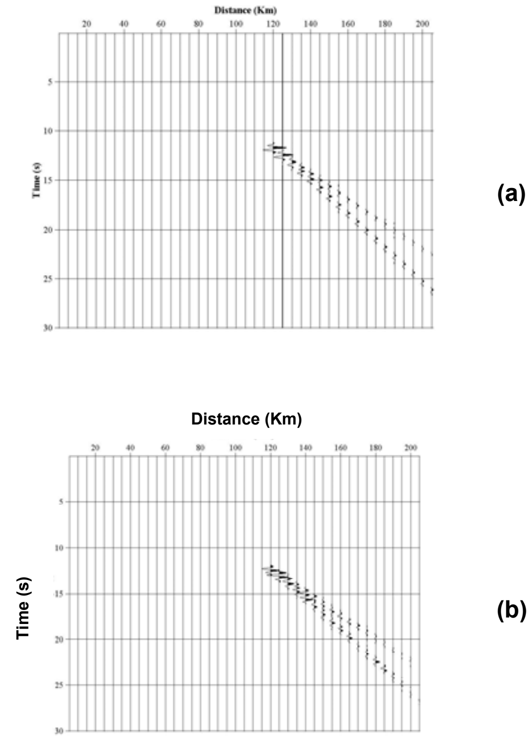

Figure 5 – Synthetic seismograms. (a) Ray theory. (b) Gaussian beam summation.

In Figure 5a we have the synthetic seismogram for the seismological experiment, obtained by the zero order ray theory solution. We can observe that at the caustic point (x = 120 Km) there is a strong amplitude anomaly, exactly where the traveltime curve (Figure 4a) diverges in two branches. In this example, due to the method itself, no observations were included in the shadow zone formed before the caustic point. This is not also observed in the case of the GBs summation (Figure 5b), but mainly this is due to the fact that we have not positioned any geophone there. On the other hand, the amplitudes observed in Figure 5b for the geophones (stations) located beyond $x >$ 120 Km also experiment an increase in their values. But in some manner this happens in a smooth way, with no phase shifts.

For comparison reasons, in Figure 6 we have depicted the values of the Fresnel zone radius, either in depth or projected towards the acquisition surface. The green triangles represent the values of the Fresnel zone radius in all depths seen by the station number 41 (x = 205 Km), while the black circles represent the values of the projected Fresnel zone for each station, respectively. The labels in red (in kilometers values), close to each curve, represent the position of each depth point with respect to each receiver. It is clear by each curve in green that the values of Fresnel zone radius decrease according to the depth. Then, the lower values of Fresnel zone radius are those referred to points belong to the depth 40 Km. In a very symmetrical way, the curves of the projected Fresnel zone radius also show a pattern according to the depth point in consideration. But as we can see in this comparison, when referred to each station, each radius (in depth or projected) present opposite values. This means that when projected towards the acquisition surface, the value in depth differ from the value projected.

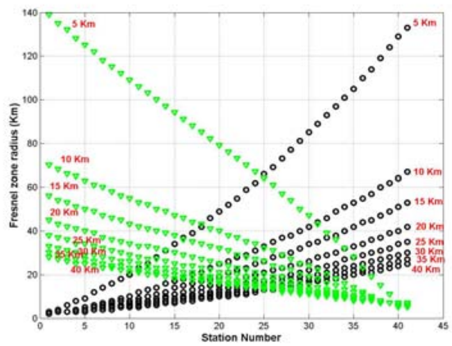

Figure 6 – Comparison of values for the Fresnel zone radius in depth (green triangles) and their respective values projected towards the acquisition surface (black circles).

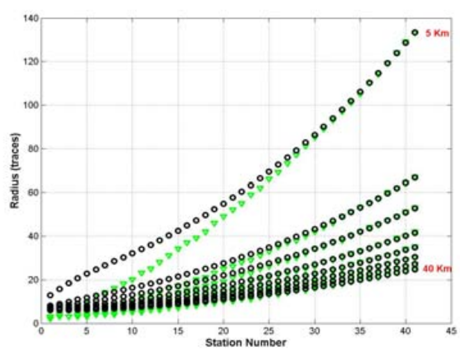

Figure 7 – Comparison of the number of traces influenced by the beam half-width (black circles) and the projected Fresnel zone radius (green triangles), both observed at receiver number 41. The values almost coincide.

Figure 7 shows a brief comparison of the number of traces influenced by the sizes (radius) of the beam half-width (black circles) and by the projected Fresnel zone radius (green triangles). The upper curve labeled 5 Km represents points belonging to this depth, while the lowest curve is the one representing depth 40 Km. The intermediate curves represent depths spaced 5 Km from each other, in a sequence. Since each receiver is spaced also 5 Km from each other, the range of some radius reaches distances of up to 700 Km, either for the projected Fresnel radius and for the beam half-width. The most representative values for both quantities are the ones belonging to depth 40 Km (less than 100 Km along the whole curve), with radius sizes lower than the dimensions of the model. Coincidently, these are places where the majority of the rays pass, and where they seem to be "reflected" from the medium, specially at depths 15 Km (near the caustic point) and 40 Km, deep inside the mantle. But the most important fact here is that these values almost coincide along the curves, which means that the constraint represented by Eq. (6) is effective and the beams at the endpoints of the rays are restricted to the projected Fresnel zone of the wavefield.

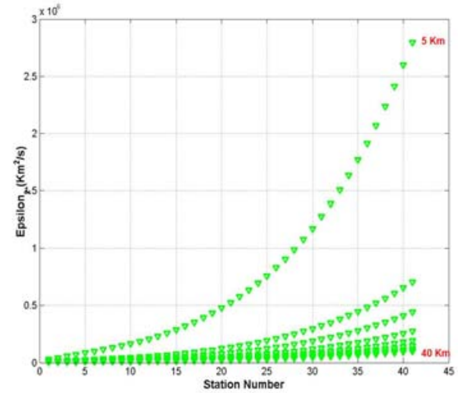

Figure 8 – Values of the parameter ε_2 for the seismological example. Only the "plus" solutions of Eq. (6) are depicted.

In this respect, we must investigate the role played by parameter ε_2 [Eq. (6)], under the condition that it grants half-widths with the most minimum value at the endpoints of the rays. In Figure 8 we have depicted these values for the receiver (station) number 41. Once restricted to the Fresnel volume, we notice that for inner depths these values are more stable and least, indicating an excellent control of the parameter. If we compare Figures 7 and 8, the beam-widths at the rayends are the least for the values of ε_2 that are more stable. This can be easily seen for the points on the curve of depth 40 Km, which yields values of beam-width less than 100 Km wide, along the whole curve (less than 20 traces of influence). This fact is in agreement with the results studied by Rüger (1993), although in the latter case the author only considered the parameter ε_2 at the source. The behaviour of the results, however, are the same and both avoid the effects observed in the modeling of the wavefield by the GB method.

Conclusions

We have studied a possible link between two quantities that have no physical relationship, but are mathematically similar. These quantities are the radius of the projected Fresnel zone (i.e., part of the Fresnel volume raytracing) and the half-width of the Gaussian beams. Gaussian beams are complex paraxial rays that are tightly concentrated close to their central rays in the meaning of Bortfeld's idea of seismic systems. One critical quantity in the description of the GBs is the determination of its half-width, a frequency dependent quantity that must be as minimum as possible along a ray. In the literature, some special conditions were studied in order to keep the half-width as minimum as possible along a given ray, but these condition could only be stated at the source and at the rays ends. This meant only and specifically a *mathematical* condition. Nothing up to now was introduced in order to constraint the wavefield described by the GBs in a *physical* way, i.e., based on quantities that physically exist and are vital to the description of the wavefield.

The Fresnel volume raytracing comes into play in the present case due to the description of a set of points over (fictitious or not) surfaces along the raypath, called Fresnel zones, and which determine a ray tube very similar to the half-width of a GB. Of course, one Fresnel zone has nothing to do with a GB half-width in a physical way, but we consider that it may serve as a strong mathematical constraint in the formation of a beam. Moreover, being projected from a to-be-imaged-reflector, towards the acqusition surface, this information could serve as input in the superposition of some several beams in order to simulate the wavefield in some given receiver and consider only those rays that are really important to consider in the superposition of beams. It is well known in the literature that a given receiver is also influenced by paraxial rays that reflect over the (first) Fresnel zone of a given reflector, and that this region over the reflector area influences in the resolution of the seismic data. In a similar way, in describing the wavefield by the superposition of GBs, only some rays in the paraxial vicinity of a central ray contribute to the observation in a given receiver. The similitude in these two ideas lead to the determination of a new weight-function in the GBs superposition, proportional to the value of the projected Fresnel zone, and that *formally* restricts the summation of rays that influences an observation at some given geophone. Then, once determined the projected Fresnel zone for each geophone, a beam parameter can be calculated and adjusted in order to keep the beam half-width as minimum as possible along the whole raypath and at the rayends.

We have tested our ideas in a single common-shot seismological model, in which we have simulated the well known situation of propogation of seismic waves through the crust-mantle interface. In the present model, one source of primary seismic waves is set and a certain number of ray is traced through a constant gradient medium simulating the crust-mantle interface. At the transition interface, the physical properties of the Earth change and make the ray refracts at the base of the simulated Moho and form a shadow zone and a divergent branch of traveltimes. With the use of the Fresnel volume elements and the constraints for the formation of the beam at the acquisition surface, we have obtained a synthetic seismogram without some artifacts and spurious arrivals. Some information was obtained in the shadow zone, but with a small amplitude, not recognized at the seismic section. The calculated beam parameter showed stable results and the half-widths were dimensionally proportional to model, yielding stable results.

Acknowledgments

The first author would like to think the Brazilian National Research Council (CNPq-Brazil), for his PhD scholarship during all the stages of this research.

References

Bortfeld, R., 1989. Geometrical ray theory: rays and traveltimes in seismic systems (second-order approximations of the traveltimes). Geophysics, **54**, 342-349.

Červený, V., 1982. Expansion of a plane wave into Gaussian beams. Studia Geoph. et Geod., **26**, 120-131.

Červený, V.; Popov, M. M.; Psencĭk, I., 1982. Computations of wavefields in inhomogeneous media – Gaussian beam approach. Geophys. J. R. astr. Soc., **70**, 109-128.

Červený, V.; Klimeš, L., 1984. Synthetic body wave seismograms for three-dimensional laterally varying media. Geophys. J. R. astr. Soc., **79,** 119-133.

Červený, V., 1985. Gaussian beam synthetic seismograms. J. Geophys., **58**, 44-72.

Červený, V., 2001. Seismic ray theory. Oxford University Press.

Ferreira, C. A. S.; Cruz, J. C. R., 2003. Comparison of ray theory, Gaussian Beam and finite-difference modeling in 2D media. 8th International Congress of the Brazilian Geophysical Society. Rio de Janeiro, Brazil.

Ferreira, C. A. S.; Cruz, J. C. R., 2004a. Modified Kirchhoff prestack depth migration using the Gaussian Beam operator as Green function. In: EAGE 66th Conference & Exhibition. Paris, France. Expanded abstracts.

Ferreira, C. A. S.; Cruz, J. C. R., 2004b. Migração pré-empilhamento em profundidade usando o operador de feixes gaussianos como função de Green – Teoria. I Workshop da Rede Cooperativa de Pesquisa em Risco Exploratório em Petróleo e Gás. Natal-RN, Brazil. Expanded abstracts.

Hubral, P.; Schleicher, J.; Tygel, M.; Hanitzsch, C., 1993. Determination of Fresnel zones from traveltime measurements. Geophysics, **58**, 703-712.

Klimeš, L., 1984. Expansion of a high-frequency time-harmonic wavefield given on an initial surface into Gaussian Beams. Geophys. J. R. astr. Soc., 79, 105-118.

Müller, G., 1984. Efficient calculation of Gaussian Beams seismograms for two-dimensional inhomogeneous media. Geophys. J. R. astr. Soc., **79**, 153-166.

Popov, M. M.; Psencĭk, I., 1978. Computation of ray amplitudes in inhomogeneous media with curved interfaces. Studia Geoph. et. Geod., **22,** 248-258.

Popov, M. M., 1982. A new method of computation of wavefields using Gaussian beams. Wave motion, **4,** 85-95.

Rüger, A., 1993. Dynamic ray tracing and its application in triangulated media. MsC thesis, Clorado School of Mines, CWP-139.

Schleicher, J.; Tygel, M.; Hubral, P., 1993. 3D true-amplitude finite-offset migration. Geophysics, **58,** 1112-1126.

Schleicher, J.; Hubral, P.; Tygel, M.; Jaya M. S., 1997. Minimum apertures and Fresnel zones in migration and demigration. Geophysics, **62**, 183-194.

Schleicher, J.; Tygel, M.; Hubral, P., 2004. True-amplitude seismic imaging. Soc. of Expl. Geophysicists. (Submitted monography).